Relaxing Conservatism for Enhanced Impedance Range and Transparency in Haptic Interaction

Huseyin Tugcan Dinc[1], *Student Member, IEEE,* Thomas Hulin[2], Christian Ott[2,3], *Member, IEEE,* and Jee-Hwan Ryu[1*], *Member, IEEE*

***Abstract*—The Time Domain Passivity Approach (TDPA) has been accepted as one of least conservative tools for designing stabilizing controllers in haptics and teleoperation, but it still suffers from conservatism because it is based on passivity. Additionally, high-frequency, immediate control actions lead to a degradation of transparency. In this paper, we propose a method to relax the conservatism of haptic interaction and enhance stable impedance range while maintaining high transparency. Based on the observation of energy exchange behavior in pressing and releasing paths in haptic interaction, we introduce an energy cycle as a completion of a pressing and releasing path. With this new concept, we compare the energies at the end of each energy cycle to estimate the energy generation and inject adaptive damping to regulate it over upcoming cycles. Because we wait a pressing-releasing cycle is completed, we allow energy to be generated, but we regulate the amount of generated energy over upcoming cycles by injecting adaptive damping. In this way, we perform low-frequency control actions on system dynamics. These in turn enable us to achieve high transparency. We show the validity of the proposed approach through several simulations and experiments, and show that it enhances the stable impedance range and transparency compared to the TDPA.**

***Index Terms*—Passivity, haptic interaction, transparency.**

I. Introduction

Among the five sensory human sensory modalities, haptic sensation is one of the most vital senses that we have. It helps us to locate objects, understand surface textures, and even can guide people, who have visual impairment, such as reading a book with their finger following the braille or walking on the street by feeling the tactile paving on pavements. Also, haptic feedback, in robotics, gives better controllability and manipulability to users, who might be performing tasks in Virtual Environments (VEs) or teleoperating a robot, because users feel the interaction forces and torques [1].

However, rendering these interaction forces and transferring them to user are not without challenges. A general haptic interaction loop consists of both mechanical and virtual elements, which include the human operator, haptic interaction device, and VE [2]. While the continuous elements, namely human operator and the mechanical parts of the haptic interaction device are assumed to be passive in the range of frequencies that we deal with, the VE exhibits active behavior due to discretization, quantization, and Zero-Order-Hold (ZOH) effects [3].

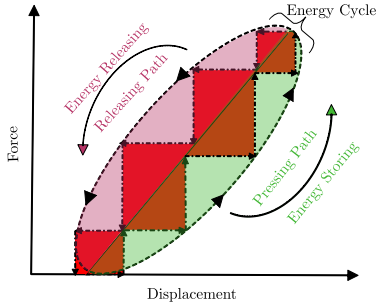

Fig. 1: Force-Displacement plot of virtual spring, showing pressing and releasing paths under the effect of Zero-Order-Hold. During the pressing path energy is being stored in the virtual spring, in the releasing path, energy is being released. An energy cycle is defined as completion of a pressing and releasing path.

While discretization involves sampling the data at constant time intervals, quantization can be thought of as sampling in amplitude. Both of these effects can lead to energy being generated (also referred to as energy leaks [4]) as shown in Fig. 1, which can potentially lead to instability, and thus endanger the illusion of reality if it is not dissipated by the intrinsic damping of the device, human arm damping [5], or a stabilizing controller.

To ensure stable haptic interaction, the widely used passivity property, while sufficient for stability, introduces conservatism, leading to performance degradation. Key factors defining haptic interaction performance are the stable impedance range (also depicted as Z-width [6]) and transparency. While impedance range refers to the bandwidth of stably renderable impedances, transparency is how well this rendering is performed or how realistically users perceive the VE, i.e., the illusion of reality. Stabilizing a system often compromises transparency, particularly when passivity is employed. In other words, stability and transparency are conflicting objectives [7].

A. State of the art

There are various analytical methods that investigate the possible virtual stiffness values that can be passively or stably rendered in haptic interaction. For the first time *Colgate and Brown* [6] revealed the dynamic range of achievable impedances, so called Z-width, that a haptic display can

This work was supported in part by the Robot Industry Core Technology Development Program (20023294) funded by the Ministry of Trade, Industry & Energy (MOTIE, Korea), and in part by the National Research Foundation of Korea under Grant NRF-2020R1A2C200416914.

∗ *Corresponding author.*

[1]Robotics Program, Korea Advanced Institute of Science and Technology (KAIST), 34141 Daejeon, South Korea. (e-mail: htdinc; jhryu@kaist.ac.kr)

[2]Institute of Robotics and Mechatronics, German Aerospace Center (DLR), 82234 Wessling, Germany. (e-mail: thomas.hulin@dlr.de)

[3]TU Wien, Automation and Control Institute (ACIN), 1040 Vienna, Austria. (e-mail: christian.ott@tuwien.ac.at)

render. They investigated the influence of velocity filtering, intrinsic dynamics, and sampling on the Z-width. Later *Hulin et al.* [5], [8] considered the influence of human operator, time delay, and physical damping and revealed passivity and stability boundaries. *Abbot and Okamura* [9] and *Diolaiti et al.* [10] thoroughly investigated the effects of discretization and quantization on virtual wall passivity and both research groups found the same condition for passive VE.

Various stabilizing control techniques have been developed to ensure stable haptic interactions and enhance renderable impedances. *Colgate et al.* proposed a virtual coupling method [11] with empirically tuned constant damping for dissipating excessive energy, while *Hannaford and Adams* extended this method to two-port networks, deriving optimal virtual coupling parameters based on haptic device dynamics [12].

Hannaford and Ryu introduced the Time Domain Passivity Approach (TDPA) to ensure passive haptic interactions by injecting adaptive damping, when necessary [13]. TDPA employs a Passivity Observer (PO) to monitor energy input-output and a Passivity Controller (PC) to inject adaptive damping based on energy generation. While TDPA is considered less conservative, it still exhibits conservatism due to its adherence to passivity, which would not allow any energy generation. Therefore, TDPA dissipates any generated energy detected by the PO and instantly activates a virtual damper that may excite high-frequency oscillations. They can lead to chattering, and thus destroy the illusion of reality [13]. Moreover, TDPA cuts down on user-perceived force, degrading transparency, and has limitations such as energy accumulation in prolonged interactions with passive VE regions and high adaptive damping in low-velocity interactions [13], [14].

B. Contributions

Previous studies usually sacrifice transparency to ensure stability in haptic interaction. Therefore, the main challenge was to enhance stable impedance range while having a transparent interaction. In this paper, we present a way out of this trade-off by introducing a method to ease the conservatism of haptic interaction with VEs. Our approach involves allowing energy generation without exciting high-frequency modes on system dynamics to achieve both high transparency and stability. We focus on the energy exchange occurring during pressing and releasing paths in haptic interaction, introducing energy cycles as the completion of these paths. Unlike TDPA, which considers passivity to guarantee stability, we present a novel concept that compares energies at the end of each energy cycle and injects adaptive damping over the respective upcoming energy cycle to regulate the generated energy. Because we wait till a pressing and releasing path is completed to regulate the generated energy, we allow energy generation over energy cycles. However, we regulate these generated energies over upcoming energy cycles by adjusting adaptive damping until generated energy is depleted i.e., system converges. This results in low-frequency modifications on the system dynamics, achieving a stable and transparent haptic interaction. In summary, we propose a less conservative stabilization approach, which in experiments can stably render up to 20 kN/m using *Omega.7* haptic device as well as maintain high transparency. As opposed to TDPA, our approach is free of energy accumulation, low velocity and chattering issues. Furthermore, similar to the TDPA, it does not require any dynamic parameter of the system to be known.

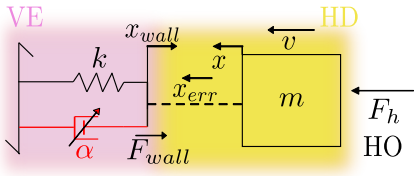

Fig. 2: A haptic interaction loop with adaptive damping α. Human operator (HO) touches the VE by using a haptic device (HD), F_h is the human force, F_{wall} is the VE reaction force, m is the inertia of the haptic device, k is the stiffness of the VE.

C. Organization of the Paper

Section II provides a brief review on TDPA. The proposed approach is detailed in Section III, with virtual wall rendering simulations in Section IV. Experimental validation and a comparison with TDPA are in Section V, while stability is discussed in Section VI. Section VII concludes the study.

II. Time-Domain Passivity Approach

TDPA consists of two elements, as briefly mentioned earlier, PO and PC. PO is used for monitoring energy input-output to the system, PC is used for injecting adaptive damping to ensure system maintains passivity all the time. In fact, to show the energy flow, for PO, we usually model a system as a network since it makes easier to understand the causality.

Assuming the initial storage of the system is $E(0)$, the one-port network is passive if and only if

$$\int_0^t f(\tau)v(\tau)\,d\tau + E(0) \geq 0, \quad \forall t \geq 0, \tag{1}$$

where f and v represent for force and velocity, respectively. According to (1), energy supplied to a passive network must be greater than negative $E(0)$ for all time [15]. The typical haptic interaction system comprises human operator, haptic interface, and VE. Both input and output variables of these elements can be measured and (1) can then be computed in real time at each time step.

Power flow is defined by discrete power conjugated pairs in a computer-controlled system. During one sampling time, the observed energy can be estimated to check the passivity of one-port networks. The observed net input energy by PO can be estimated as follows:

$$E_{\text{obs}}(n) = \Delta T \sum_{i=0}^{n} f(t_i)v(t_i) \tag{2}$$

where ΔT is the sampling period and $t_i = i \times \Delta T$. If the observed energy is greater than zero, it indicates that the system does not generate energy. If there is a moment

that observed energy becomes smaller than zero, it indicates that the system generates energy. Because we are aware of the amount of generated energy, we can dissipate that excessive energy by injecting appropriate PC depending on input causality [13].

As per causality of an one-port network, PC can be either of impedance or admittance type. In impedance configuration (what we focus in this work), velocity is maintained across network ports while a damping force is added to dissipate the energy. The adaptive damping gain for impedance causality is

$$\alpha(n) = \begin{cases} -E_{\text{obs}}(n)/(\Delta T v(t_n)^2) & E_{\text{obs}}(n) < 0 \\ 0 & E_{\text{obs}}(n) \geq 0 \end{cases} \tag{3}$$

III. Proposed Approach

While TDPA is considered less conservative among passivity-based methods, it still relies on passivity conditions for stability and does not allow for energy generation. TDPA instantly dissipates any generated energy and cuts down the user-perceived force with high-frequency control actions, causing sustained vibrations and potential instabilities, especially in systems with fast dynamics, e.g., high stiffness rendering. Consequently, achieving both high impedance range and transparency in haptic interaction becomes challenging.

However, allowing energy generation while maintaining stability enables a higher impedance range and more transparent haptic interaction. Based on the observation of pressing and releasing paths during haptic interaction (Section III-A will highlight this important observation on the energy exchange in Human-Robot Interaction (HRI) tasks), we introduce two different concepts, namely energy exchange and energy cycles. These concepts provide two advantages—permitting energy generation during interaction in contrast to passivity and regulating this energy smoothly through low-frequency modifications. Consequently, rendering high stiffness values becomes achievable while maintaining high transparency in the interaction.

A. Energy Exchange

In HRI, we generally experience repetitive in-out motion that leads to continuous storing and releasing energy e.g., energy is being transferred from one component to another. In haptics, energy exchange happens between Human Operator (HO), Haptic Device (HD), and VE while in teleoperation energy exchange occurs in the order HO, HD, communication channel, remote device and finally environment and is reflected back to HO in the reverse order for both cases. The question for us was how should we understand the energy exchange in these systems and deduce a meaningful outcome?

In networked systems, a positive sign of the product of power-conjugate pairs means that energy is being stored in the system, and a negative sign signifies that energy is being released from the network. From the difference between released and stored energy, the amount of energy being generated or dissipated can be derived.

A human operator interacting with a VE using a haptic device is illustrated in Fig. 2. Basically, the HO pushes with the force F_h on a HD, which has an inertia m and hence gains a velocity v. Once the difference between the HD position x and the virtual wall position x_{wall} is smaller than zero (i.e., $x_{\text{err}} = x - x_{\text{wall}}$), the HO feels a reaction force F_{wall}. The governing equation of the illustrated system (when there is no damping) is written as

$$\ddot{x} = \dot{v} = \frac{F_h - F_{\text{wall}}}{m}, \tag{4}$$

where

$$F_{\text{wall}} = \begin{cases} -kx_{\text{err}} & x_{\text{err}} < 0 \\ 0 & x_{\text{err}} \geq 0 \end{cases} \tag{5}$$

Once we look at the energy behavior of the VE in Fig. 2, we see that energy storage starts with the pressing path. Basically, the virtual spring stores energy in this stage, so the VE experiences positive power. Then, energy release starts with the releasing path in which the virtual spring releases its stored energy, resulting in the VE experiencing negative power. Note that the HO does not necessarily interact with the VE in a specific pattern to produce pressing and releasing paths. The nature of the haptic interaction with the VE usually leads to multiple pressing and releasing paths. The total energy of the VE can be written as

$$E_{\text{tot}} = E_{\text{sto}} + E_{\text{diss}} + E_{\text{gen}}, \tag{6}$$

where E_{sto} is the energy stored by the spring, E_{diss} is the energy dissipated by the damping of VE, HD, and HO, and E_{gen} is the energy generated due to effects such as discretization and quantization. In stable systems, energy storing and releasing continuously follow each other until the system reaches its equilibrium point i.e., system does not have any energy to release. In this work, in the sense of energy exchange, we aim to estimate E_{gen} to achieve stable haptic interaction.

B. Energy Cycle

The phenomena that we called as 'energy exchange' leads us to define energy cycles. We name the completion of a pressing and releasing path as an energy cycle (see Fig. 1). Upon completion of a pressing and releasing paths, we can refer to this as one energy cycle being completed. Based on the energy levels at the end of each energy cycle, we could estimate energy generation E_{gen}. Thereby, if we detect any generated energy, we inject adaptive damping over the next cycle in order to smoothly regulate energy generation over upcoming energy cycles. In addition, adaptive damping can be adjusted over each energy cycle depending on the amount of generated energy.

The naive idea of defining energy cycles is to investigate when the position error (x_{err}) of the system becomes zero. In general, however, the haptic interaction leads to a displacement so that convergence takes place inside the virtual wall. To detect energy cycles, we have to find the moment when the power sign changes from negative to positive – the energy releasing phase ends and energy storing phase starts. The primary goal is to pinpoint this moment in time. Fig. 3 illustrates typical position, energy, and power signals during haptic interaction with a virtual wall (i.e., system in Fig. 2 with no adaptive damping).

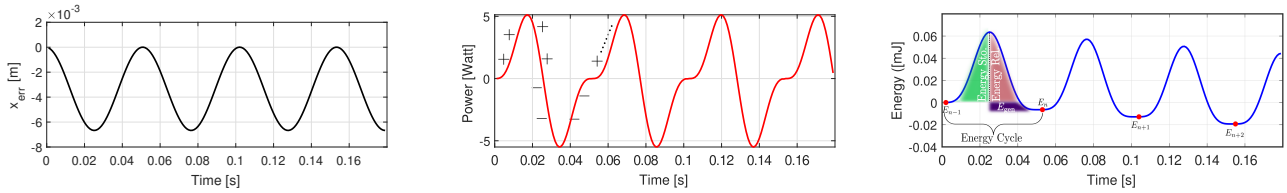

(a) (b) (c)

Fig. 3: (a) Displacement of VE (of system in Fig. 2) with $k = 3$ kN/m, $b = 0$ Ns/m, (b) Power and, (c) energy behavior of virtual spring. When power positive, energy stored in the spring (green area), and when it is negative energy releasing from the spring (red area). Due to effects such as discretization and quantization, energy is generated (purple area) at the end of each energy cycle.

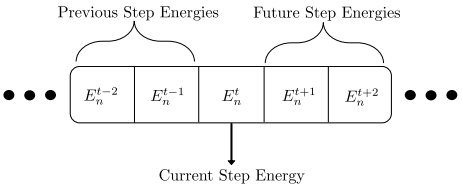

Fig. 4: The time-window in order to avoid fault detection of energy cycles.

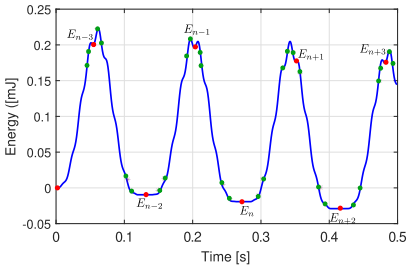

Fig. 5: Noisy energy signal with some incorrectly detected energy cycles (red). Upon detection of an energy cycle, the time window compares it with two previous and future steps energy values (green) whether it is true an energy cycle.

During the pressing path, positive power signifies energy storage, and during the releasing path, negative power indicates energy release. The cycle repeats until the system converges or diverges. The ZOH effect (see Fig. 1) causes the released energy to exceed the stored energy, leading to active behavior. The amount of generated energy E_{gen} is the difference between the energies at the end of subsequent energy cycles, which is illustrated in Fig. 3c and can be calculated as

$$E_{\text{gen},n} = E_n - E_{n-1}, \tag{7}$$

where E_{n-1} and E_n are energies at the end of the $(n-1)$th and nth energy cycles, and $E_{\text{gen},n}$ is the generated energy at the end of the nth cycle. As generated energy may vary across cycles, adaptive damping adjusts to regulate it. Utilizing $E_{\text{gen},n}$, we calculate the required adaptive damping for the $(n+1)$th cycle to regulate energy generation (see Fig. 3c) as

$$\alpha_c^n = \alpha_c^{n-1} + \frac{-E_{\text{gen},n}}{\sum_{n-1}^{n} v^2 \Delta T}, \tag{8}$$

where α_c^n is the adaptive damping that is calculated at the end of nth cycle for the $(n+1)$th cycle, α_c^{n-1} is adaptive damping from the previous energy cycle ($(n-1)$th), v is the velocity, ΔT is the sampling period. Our virtual wall equation with adaptive damping α_c shown in (9).

$$F_{\text{wall}} = \begin{cases} -kx_{\text{err}} - \alpha_c^n \dot{x}_{\text{err}} & x_{\text{err}} < 0 \\ 0 & x_{\text{err}} \geq 0 \end{cases} \tag{9}$$

The calculation of adaptive damping in our approach is akin to TDPA with one major difference. In TDPA, the damping force is designed to immediately dissipate the observed energy as soon as it exceeds a threshold value, which leads to high-frequency control actions. In contrast, our approach computes the necessary damping at the end of each energy cycle, modifying system dynamics for the following cycle. This distribution of adaptive damping effects throughout the complete energy cycle makes our controller less aggressive than TDPA, eliminating chattering. Moreover, as our method observes energies only at the end of cycles, it avoids energy accumulation.

C. Time-Window

Although detecting energy cycles theoretically seems straightforward, in practice, it poses challenges. Accurate detection of cycles, especially at the end of each releasing path, requires careful monitoring of power sign changes. The noisy nature of power conjugate pairs, force and velocity, due to integration and digital computations in the discrete domain complicates this process. Initial attempts using power sign changes led to faulty cycle detection, as small and noisy changes were erroneously considered as energy storing and releasing behavior (see Section V Fig. 7). These noisy power signal changes, resulting from digital computations, do not accurately represent actual pressing and releasing paths. Therefore, a method needs to be developed to prevent incorrect detection of energy cycles caused by the noisy power signal.

In order to avoid false detection, we utilize so called time-window technique, similar to the one in [16]. In our time-window technique (see Fig. 4), we save the energy values within some previous and future steps and we know that after actual energy releasing occurs, energy storing should start for the sake of energy exchange. We can monitor whether this condition is satisfied by comparing the energy values that we saved in the time-window. Note that the time-window does not

act as a low-pass filter, which would change the magnitude of the signal. To show how time-window approach works, a scenario is illustrated in Fig. 5 with a noisy energy signal. After detecting an energy cycle, time-window compares it with previous and future steps energy values (green points in Fig. 5). The following condition must be satisfied so that, e.g. in the case of E_{n-1}, an actual energy cycle is completed:

$$\dots \; E_{n-1}^{t-2} > E_{n-1}^{t-1} > E_{n-1}^{t} < E_{n-1}^{t+1} < E_{n-1}^{t+2} \; \dots \tag{10}$$

where E_{n-1}^{t-2} and E_{n-1}^{t-1} are two time steps previous, and E_{n-1}^{t+1} and E_{n-1}^{t+2} are two time steps future energy values. For the sake of energy exchange, energy should decrease (releasing path) before actual energy cycle, and increase (pressing path) after it. Therefore, the time-window eliminates E_{n-3}, E_{n-1}, E_{n+1}, and E_{n+3}, but selects E_{n-2}, E_n, and E_{n+2} as actual energy cycles.

Due to the time-window, the injection of the adaptive damping would be delayed as amount of future steps for each energy cycle. In this respect, the delayed damping that is injected in the nth energy cycle is applied until $(n+1)$th energy cycle adaptive damping injected. Therefore, the delay of adaptive damping in the current energy cycle would be compensated in the upcoming energy cycle.

If the upcoming energy cycle's velocity profile significantly differs from the current one, adaptive damping may not sufficiently dissipate energy. Increasing the time-window size exacerbates this dissipation shortfall. Despite the method focusing on regulating energy generation at cycle ends, the system's convergence time would be prolonged due to dissipation deficiency. This relation is crucial in determining the time-window size.

Based on our observation the actual sign change of power signal happens in one or two steps in 1 ms sampling period. The determination of the size of the time-window depends on the sampling period and noise level of the force and velocity signal, and the total inertia of the haptic device during the interaction with the HO. In this stage of our work, the size of the time-window is determined heuristically. The size of the previous and future steps may be different, but it seems advisable to use the same size to obtain a symmetrical comparison, as in Fig. 5.

IV. Simulating Virtual Walls

We conducted simulations to illustrate the working principle and feasibility of our approach, testing it under various virtual wall conditions. Fig. 2 demonstrates a general haptic interaction case, while Fig. 3b and 3c display the energy and power behavior of this haptic interaction system. Due to the active nature of a typical virtual spring, energy values at the end of each energy cycle decrease, as shown in Fig. 3c. This is because the released energy surpassing the stored energy. Without injecting the necessary adaptive damping to regulate generated energies at the end of each cycle, oscillations occur, disrupting the illusion of reality for haptic interaction.

The haptic system in Fig. 2, with the proposed controller, applies damping when E_{gen} is detected at the end of an energy cycle, regulating energy generation in the next cycle (using (9)). Engaging our controller injects damping at the end of each energy cycle, preventing released energy from exceeding stored energy which regulates released energy from becoming bigger than stored energy i.e., it regulates energy generation as shown in Fig. 6. Two simulation sets demonstrate the approach. In the first set (Fig. 6a, 6b, 6c), a virtual spring ($k = 3$ KN/m) without additional damping (0 Ns/m) achieves stable haptic interaction with the engagement of adaptive damping. In the second set (Fig. 6d, 6e, 6f), maintaining the same virtual spring, negative damping (-1.0 Ns/m) is added after $0.2s$ to demonstrate the approach's robustness. The method successfully regulates energy generation, converging position in both sets.

V. Experiments

We tested the validity of the proposed method using an *Omega.7* haptic device with different stiffness conditions of the VE. In the current stage of our research, we only tested the proposed approach with single axis to show the core working concept. A virtual wall is placed on the xy plane (parallel to device base), so HO approaches to the virtual wall in the $-z$ axis. The *Omega.7* haptic device can render 8 kN/m without any external passivation approach. Therefore, we set the virtual spring stiffness $k = 12$ kN/m, which is higher than the upper limit of the device.

As we experimented single-dof (degree of freedom) haptic interaction, the power signal was noisy similar to what we simulated in the previous section. The noisy power signal leads our algorithm to detect false sign changes as energy cycles as shown in Fig. 7, resulting in false adaptive damping adjustments. Typically, this causes system instabilities as adaptive damping adjustments are not grounded in true energy cycles. To address this, we activate the time-window alongside our algorithm.

Position and energy signals are shown in Fig. 8 with the time-window in operation. Time-window uses two steps of previous and two steps of future energy values to determine actual energy cycles. The width of the time-window is determined experimentally. As power sing changes occurs in one or two steps in 1ms sampling period, we agreed on total five steps of time-window (two steps previous, two steps future, and the current value) is appropriate for various VEs (e.g. various stiffness values).

Without a controller (Fig. 8), users experience oscillations, preventing stable interaction. To validate our method, we conducted experiments with varying virtual wall stiffness using the *Omega.7* haptic device. In the first set (Fig. 9a, 9d, 9g, 9j), stable interaction is achieved with $k = 12$ kN/m; the controller adjusts adaptive damping for energy cycle regulation. In the second (Fig. 9b, 9e, 9h, 9k) and third (Fig. 9c, 9f, 9i, 9l) sets, energy cycles are bounded to previous ones due to adaptive damping adjustments. The proposed method ensures stable interaction up to 20 kN/m.

To compare with TDPA [13], an experiment with $k = 12$ kN/m is conducted (Fig. 10). Despite TDPA not allowing energy generation below zero threshold, it fails to maintain

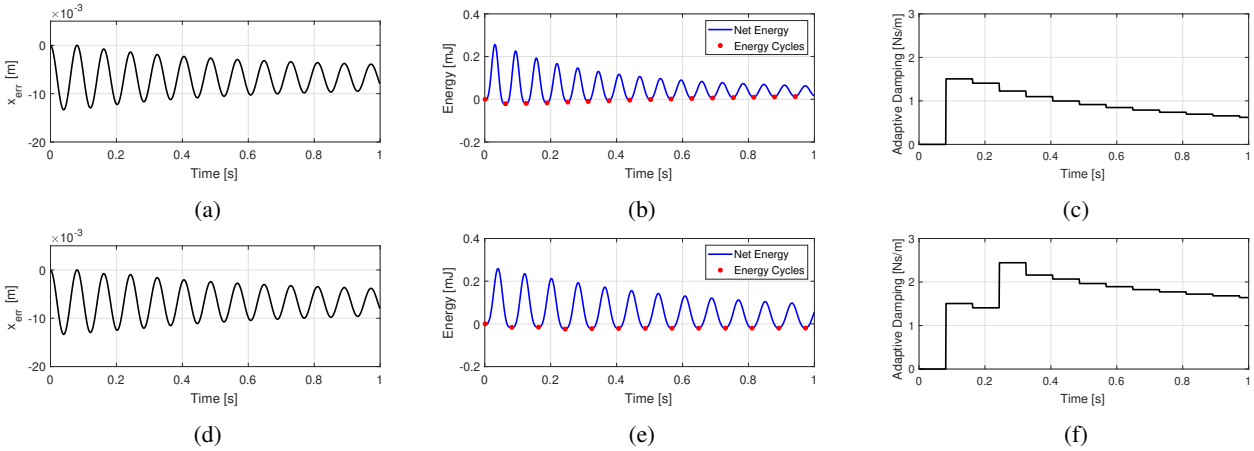

Fig. 6: Simulation results of interacting VE with $k = 3$ kN/m with inertia of HD is $m = 0.5$ kg for (a) position, (b) energy, and (c) adaptive damping. Upon detection of generated energy, 'E_{gen}', adaptive damping is engaged and it is prevented energy generation over the upcoming cycles, hence position starts to converge. For the set of (d), (e), and (f) virtual spring was set to $k = 3$ kN/m but after 0.2 s an additional constant negative damping (-1 Ns/m) is engaged to the system to show the robustness of the proposed controller.

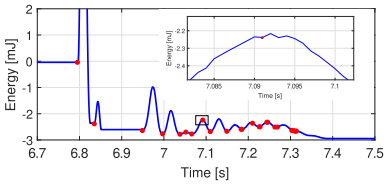

Fig. 7: Experimental result without time-window. There are multiple incorrect detections of energy cycles, which breaks the illusion of reality.

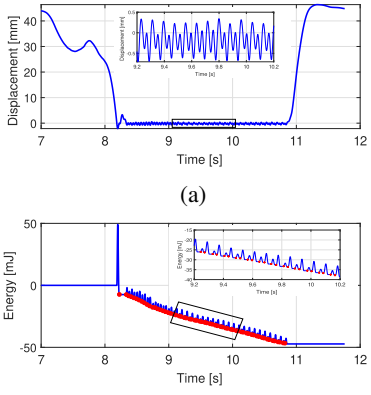

Fig. 8: Experimental result with $k = 12$ kN/m without proposed controller.

stability with the applied stiffness value due to its high-frequency modification nature. Waiting until energy crosses zero threshold results in instant modifications, preventing stable interaction with fast dynamic ranges i.e., high stiffness values.

Examining the energy signal in Fig. 9, the proposed approach differs from passivity-based methods such as TDPA. It permits energy generation below the zero threshold by regulating energy between energy cycles, relaxing the conservatism of haptic interaction. This improvement allows rendering stable high stiffness values, reaching up to 20 kN/m. Additionally, unlike TDPA (Fig. 10d) the proposed approach achieves transparent interaction, as demonstrated in Fig. 11. Displayed stiffness, which is the ratio of virtual wall force F_{wall} over displacement error x_{err}, converges to desired stiffness, while maintaining stable high stiffness rendering.

VI. Stability of Proposed Approach

The proposed controller deviates from the established passivity condition as it actively generates energy. We demonstrate stability of the system in Fig. 2 by constraining the generated energy within a finite range, preventing from escalating infinitely. Consequently, the proposed controller achieves stability in the context of Input-to-State Stability (ISS) [17], [18]. Consider the scenario where the energy produced by a system can be constrained by the summation of the square of velocity multiplied by a negative constant

$$\sum_{T_1}^{T_n} F_{\text{wall}} \dot{x}_{\text{err}} \Delta T \geq -\alpha_{\max} \sum_{T_1}^{T_n} \dot{x}_{\text{err}}^2 \Delta T, \tag{11}$$

which implies that we can posit the existence of a consistently finite digital damping value $\alpha_{\max}$ [5] that serves to dissipate the energy generated by the system. The lower and upper bounds of the $\sum$ operation refer to start and end of the corresponding energy cycle and their time stamps. The produced energy for the upcoming energy cycle $(n+1)$th is

$$\begin{aligned} &\sum_{T_1}^{T_n} F_{\text{wall}} \dot{x}_{\text{err}} + \sum_{T_n+\Delta T}^{T_{n+1}} (F_{\text{wall}} - \alpha_c^n \dot{x}_{\text{err}}) \dot{x}_{\text{err}} \geq \\ &- \alpha_{\max} \sum_{T_1}^{T_n} \dot{x}_{\text{err}}^2 - \alpha_{\max} \sum_{T_n+\Delta T}^{T_{n+1}} \dot{x}_{\text{err}}^2. \end{aligned} \tag{12}$$

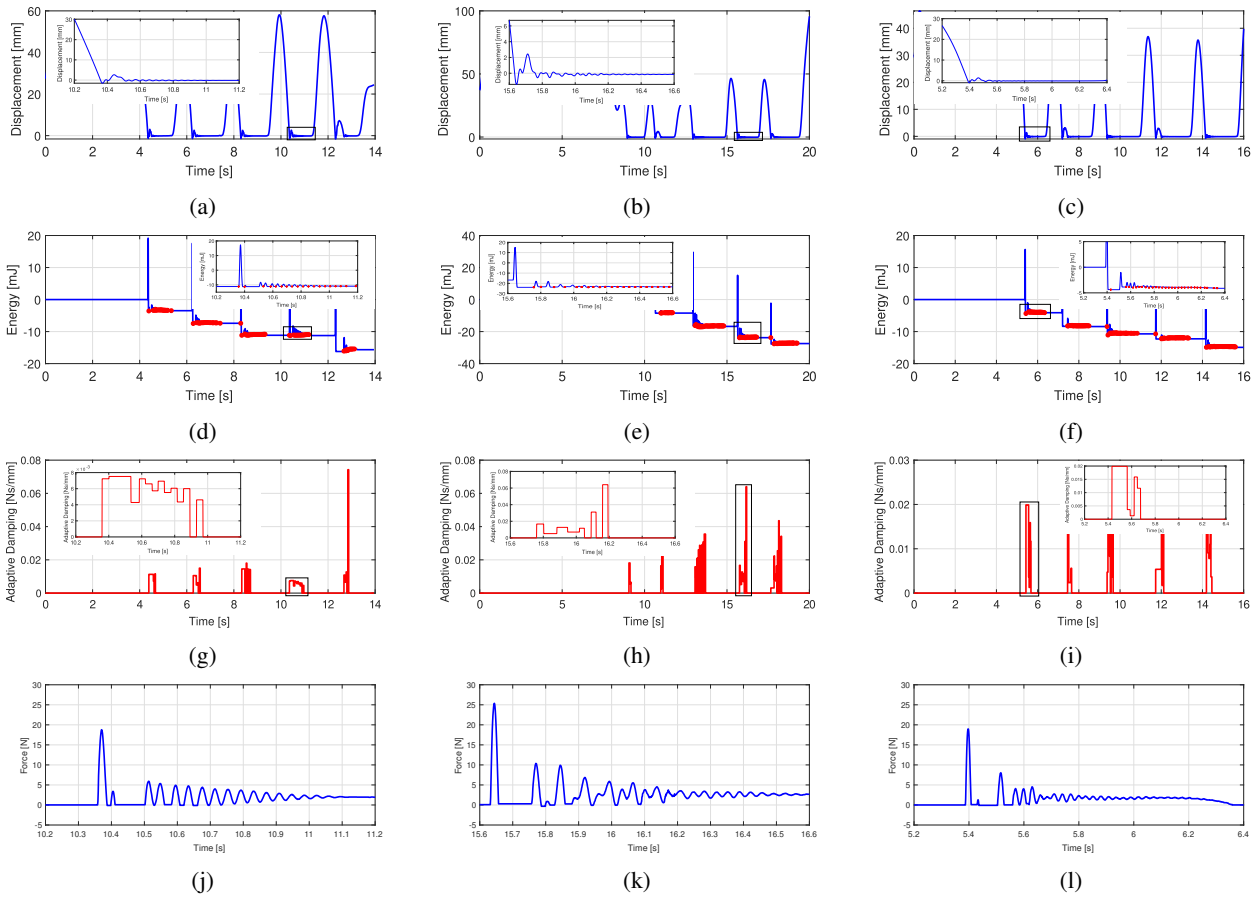

Fig. 9: Results of the experiments with different virtual spring values using proposed method. The first row stands for positions (x_{err} with $x_{\text{wall}} = 0$), the second row is for energy (E_{tot}), the third row is for adaptive damping (α), and the fourth row is for force (F_{wall}). Each column represents an experiment. In the first experiment [(a), (d), (g), (j)] k is set to 12 kN/m, in second experiment [(b), (e), (h), (k)] k is set to 18 kN/m. and in the third experiment [(c), (f), (i), (l)] k is set to 20 kN/m.

where $(T_n + \Delta T)$ is the starting time-stamp of the nth energy cycle. Then, the produced energy until $(n+1)$th energy cycle becomes

$$\sum_{T_1}^{T_{n+1}} F_{\text{wall}}\dot{x}_{\text{err}} \geq -\alpha_{\max}\sum_{T_1}^{T_n}\dot{x}_{\text{err}}^2 \overbrace{-(\alpha_{\max}-\alpha_c^n)}^{\lambda_1}\sum_{T_n+\Delta T}^{T_{n+1}}\dot{x}_{\text{err}}^2. \quad (13)$$

And it is calculated for $(n+2)$th cycle as

$$\sum_{T_1}^{T_{n+2}} F_{\text{wall}}\dot{x}_{\text{err}} \geq -\alpha_{\max}\sum_{T_1}^{T_n}\dot{x}_{\text{err}}^2 - \lambda_1 \overbrace{-(\alpha_{\max}-\alpha_c^{n+1})}^{\lambda_2}\sum_{T_{n+1}+\Delta T}^{T_{n+2}}\dot{x}_{\text{err}}^2. \quad (14)$$

Finally, for the $(k+1)$th cycle ($k \geq n$), it holds

$$\sum_{T_1}^{T_{k+1}} F_{\text{wall}}\dot{x}_{\text{err}} \geq -\alpha_{\max}\sum_{T_1}^{T_n}\dot{x}_{\text{err}}^2 - \lambda_1 - \lambda_2 \ldots\ldots - \underbrace{(\alpha_{\max}-\sum\alpha_c^k)}_{=0}\sum_{T_k+\Delta T}^{T_{k+1}}\dot{x}_{\text{err}}^2. \quad (15)$$

During the interaction, in the worst-case scenario, when energy is produced in every energy cycle, as in (8), it is expected that $\alpha_c^k = \sum_{j=0}^{k}\alpha_c^{n+j} \Rightarrow \alpha_{\max}$ as $k \Rightarrow \infty$. Thus, (15) becomes

$$\sum_{T_1}^{T_{k+1}} F_{\text{wall}}\dot{x}_{\text{err}} \geq -\text{finite}. \quad (16)$$

In the worst-case scenario, with the proposed controller, the total generated energy (as in (16)) will be lower bounded by a finite amount of energy and the system remains ISS [19].

VII. Conclusion

In this study, we present a method to relax conservatism in haptic interaction to achieve higher impedance range and transparency. Based on the energy exchange behavior of haptic interaction, utilization of energy cycles allow energy generation, which relax the conservatism of the interaction. Low-frequency control actions using adaptive damping regulates energy generation through energy cycles, which enable us to achieve stability as well as high transparency.

The presented method, unlike TDPA, is free of energy accumulation and chattering problem, which give it a big potential to be applied to various systems. Because they exhibit

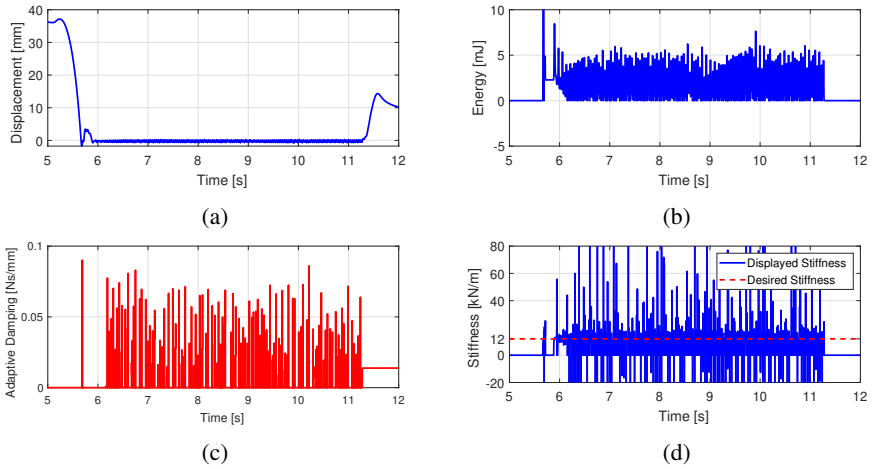

Fig. 10: Experimental result for interaction with virtual wall ($k = 12$ kN/m) using TDPA.

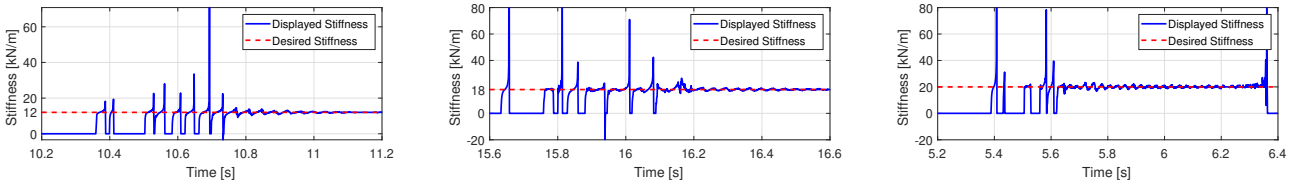

Fig. 11: Displayed stiffness values of the proposed approach for (a) $k = 12$ kN/m, (b) $k = 18$ kN/m, and (c) $k = 20$ kN/m.

an energy exchange behavior as presented in this paper, the proposed method can also be applied to time-delayed teleoperation and stable rigid contact interaction with admittance-controlled robots. As a future work, we aim to extend this approach to interaction with complex VE, multi-dof haptic interaction and teleoperation. We also plan to work on research into the reliable detection of energy cycles, specifically by means of suitable signal filtering.

REFERENCES

[1] K. Hashtrudi-Zaad and S. E. Salcudean, "Transparency in time-delayed systems and the effect of local force feedback for transparent teleoperation," *IEEE Trans. on Robotics and Automation*, vol. 18, no. 1, pp. 108–114, 2002.

[2] B. Hannaford and A. M. Okamura, *Haptics*. Cham: Springer International Publishing, 2016, pp. 1063–1084. [Online]. Available: https://doi.org/10.1007/978-3-319-32552-1_42

[3] J.-H. Ryu *et al.*, "Sampled and continuous time passivity and stability of virtual environments," in *IEEE ICRA*, Sep. 2003, pp. 822–827.

[4] R. B. Gillespie, M. R. Cutkosky *et al.*, "Stable user-specific haptic rendering of the virtual wall," in *ASME Int. Mechanical Engineering Congress and Exhibition*, vol. 58, 1996, pp. 397–406.

[5] T. Hulin, A. Albu-Schäffer, and G. Hirzinger, "Passivity and stability boundaries for haptic systems with time delay," *IEEE Trans. on Control Systems Technology*, vol. 22, no. 4, pp. 1297–1309, Jul. 2014.

[6] J. E. Colgate *et al.*, "Factors affecting the z-width of a haptic display," in *IEEE ICRA*, May 1994, pp. 3205–3210.

[7] D. A. Lawrence, L. Y. Pao, M. A. Salada, and A. M. Dougherty, "Quantitative experimental analysis of transparency and stability in haptic interfaces," in *Proc. Fifth Annual Symposium on Haptic Interfaces for Virtual Environment and Teleoperator Systems*. Citeseer, 1996, pp. 441–449.

[8] T. Hulin, "A practically linear relation between time delay and the optimal settling time of a haptic device," *IEEE Robotics and Automation Letters*, vol. 2, no. 3, pp. 1632–1639, 2017.

[9] J. J. Abbott and A. M. Okamura, "Effects of position quantization and sampling rate on virtual-wall passivity," *IEEE Trans. on Robotics*, vol. 21, no. 5, pp. 952–964, Oct. 2005.

[10] N. Diolaiti *et al.*, "Stability of haptic rendering: Discretization, quantization, time delay, and coulomb effects," *IEEE T-RO*, vol. 22, no. 2, pp. 256–268, 2006.

[11] J. E. Colgate *et al.*, "Issues in the haptic display of tool use," in *IEEE IROS*, vol. 3, Pittsburgh, PA, USA, Aug 1995, pp. 140–145.

[12] R. J. Adams and B. Hannaford, "Stable haptic interaction with virtual environments," *IEEE Trans. on Robotics and Automation*, vol. 15, no. 3, pp. 465–474, 1999.

[13] B. Hannaford and J.-H. Ryu, "Time-domain passivity control of haptic interfaces," *IEEE Trans. on Robotics and Automation*, vol. 18, no. 1, pp. 1–10, Feb. 2002.

[14] J.-H. Ryu, C. Preusche, B. Hannaford, and G. Hirzinger, "Time domain passivity control with reference energy behavior," *IEEE Trans. on Control Systems Technology*, vol. 13, no. 5, pp. 737–742, Sep. 2005.

[15] J. C. Willems, "Dissipative dynamical systems part i: General theory," *Archive for rational mechanics and analysis*, vol. 45, no. 5, pp. 321–351, 1972.

[16] A. Campeau-Lecours, M. Otis, P.-L. Belzile, and C. Gosselin, "A time-domain vibration observer and controller for physical human-robot interaction," *Mechatronics*, vol. 36, pp. 45–53, 2016.

[17] E. D. Sontag and Y. Wang, "On characterizations of the input-to-state stability property," *Systems & Control Letters*, vol. 24, no. 5, pp. 351–359, 1995.

[18] E. D. Sontag, *Input to State Stability: Basic Concepts and Results*. Berlin, Heidelberg: Springer Berlin Heidelberg, 2008, pp. 163–220. [Online]. Available: https://doi.org/10.1007/978-3-540-77653-6_3

[19] A. Jafari *et al.*, "The input-to-state stable (iss) approach for stabilizing haptic interaction with virtual environments," *IEEE T-RO*, vol. 33, no. 4, pp. 948–963, 2017.